



Published in final edited form as:

N Engl J Med. 2015 June 25; 372(26): 2481–2498. doi:10.1056/NEJMoa1402121.

Comprehensive, Integrative Genomic Analysis of Diffuse Lower-Grade Gliomas

The Cancer Genome Atlas Research Network*

Abstract

BACKGROUND—Diffuse low-grade and intermediate-grade gliomas (which together make up the lower-grade gliomas, World Health Organization grades II and III) have highly variable clinical behavior that is not adequately predicted on the basis of histologic class. Some are indolent; others quickly progress to glioblastoma. The uncertainty is compounded by interobserver variability in histologic diagnosis. Mutations in *IDH*, *TP53*, and *ATRX* and codeletion of chromosome arms 1p and 19q (1p/19q codeletion) have been implicated as clinically relevant markers of lower-grade gliomas.

METHODS—We performed genomewide analyses of 293 lower-grade gliomas from adults, incorporating exome sequence, DNA copy number, DNA methylation, messenger RNA expression, microRNA expression, and targeted protein expression. These data were integrated and tested for correlation with clinical outcomes.

RESULTS—Unsupervised clustering of mutations and data from RNA, DNA-copy-number, and DNA-methylation platforms uncovered concordant classification of three robust, nonoverlapping, prognostically significant subtypes of lower-grade glioma that were captured more accurately by *IDH*, 1p/19q, and *TP53* status than by histologic class. Patients who had lower-grade gliomas with an *IDH* mutation and 1p/19q codeletion had the most favorable clinical outcomes. Their gliomas harbored mutations in *CIC*, *FUBP1*, *NOTCH1*, and the *TERT* promoter. Nearly all lower-grade gliomas with *IDH* mutations and no 1p/19q codeletion had mutations in *TP53* (94%) and *ATRX* inactivation (86%). The large majority of lower-grade gliomas without an *IDH* mutation had genomic aberrations and clinical behavior strikingly similar to those found in primary glioblastoma.

CONCLUSIONS—The integration of genomewide data from multiple platforms delineated three molecular classes of lower-grade gliomas that were more concordant with *IDH*, 1p/19q, and *TP53* status than with histologic class. Lower-grade gliomas with an *IDH* mutation either had 1p/19q codeletion or carried a *TP53* mutation. Most lower-grade gliomas without an *IDH* mutation were molecularly and clinically similar to glioblastoma. (Funded by the National Institutes of Health.)

Address reprint requests to Dr. Daniel J. Brat at the Department of Pathology and Laboratory Medicine, Winship Cancer Institute, Emory University Hospital, G-167, 1364 Clifton Rd. N.E., Atlanta, GA 30322, or at dbrat@emory.edu.

*The authors are members of the Cancer Genome Atlas Research Network, and their names, affiliations, and roles are listed in Supplementary Appendix 1, available at NEJM.org

The authors' full names and academic degrees are listed in the Appendix.

The views expressed in this article are those of the authors and do not reflect the official policy of the National Institutes of Health.

Disclosure forms provided by the authors are available with the full text of this article at NEJM.org.

Diffuse low-grade and intermediate-grade gliomas (World Health Organization [WHO] grades II and III, hereafter called lower-grade gliomas) (see the Glossary) are infiltrative neoplasms that arise most often in the cerebral hemispheres of adults and include astrocytomas, oligodendrogliomas, and oligoastrocytomas.^{1,2} Because of their highly invasive nature, complete neurosurgical resection is impossible, and the presence of residual tumor results in recurrence and malignant progression, albeit at highly variable intervals. A subset of these gliomas will progress to glioblastoma (WHO grade IV gliomas) within months, whereas others remain stable for years. Similarly, survival ranges widely, from 1 to 15 years, and some lower-grade gliomas have impressive therapeutic sensitivity.^{3–5} Current treatment varies with the extent of resection, histologic class, grade, and the results of ancillary testing and includes clinical monitoring, chemotherapy, and radiation therapy, with salvage options available in the event of treatment failure.^{6–8}

Although the histopathological classification of lower-grade gliomas is time-honored, it suffers from high intraobserver and interobserver variability and does not adequately predict clinical outcomes.^{9,10} Consequently, clinicians increasingly rely on genetic classification to guide clinical decision making.^{11–14} Mutations in *IDH1* and *IDH2* (two very similar genes, hereafter referred to collectively as *IDH*) characterize the majority of lower-grade gliomas in adults and define a subtype that is associated with a favorable prognosis.^{15–17} Lower-grade gliomas with both an *IDH* mutation (i.e., a mutation in either *IDH1* or *IDH2*) and deletion of chromosome arms 1p and 19q (1p/19q codeletion), which occurs most often in oligodendrogliomas, have better responses to radiochemotherapy and are associated with longer survival than diffuse gliomas without these alterations.^{5,18} *TP53* and *ATRX* mutations are more frequent in astrocytomas and are also important markers of clinical behavior.¹⁹ To gain additional insight, we performed a comprehensive, integrative analysis of 293 lower-grade gliomas from adults, using multiple advanced molecular platforms. We performed an unsupervised analysis of integrated whole-genome molecular data to determine whether we could identify biologic classes of disease with clinically distinct behavior and to determine whether these classes were captured more accurately by molecular-marker status than by histologic class.

METHODS

PATIENTS

The tumor samples we analyzed were from 293 adults with previously untreated lower-grade gliomas (WHO grades II and III), including 100 astrocytomas, 77 oligoastrocytomas, and 116 oligodendrogliomas. Pediatric lower-grade gliomas were excluded; their molecular pathogenesis is distinct from that of lower-grade gliomas in adults.^{20,21} Diagnoses were established at the contributing institutions; neuropathologists in our consortium reviewed the diagnoses and ensured the quality of the diagnoses and of the tissue for molecular profiling (see Supplementary Appendix 1, available with the full text of this article at NEJM.org, for sample inclusion criteria). Patient characteristics are described in Table 1, and in Table S1 (Supplementary Appendix 2) and Table S2 in Supplementary Appendix 1. We obtained appropriate consent from relevant institutional review boards, which coordinated the consent process at each tissue-source site; written informed consent was obtained from all

participants. The patients' ages, tumor locations, clinical histories and outcomes, tumor histologic classifications, and tumor grades were typical of adults with a diagnosis of diffuse glioma.^{1,2}

ANALYTIC PLATFORMS

We performed exome sequencing (289 samples), DNA copy-number profiling (285), messenger RNA (mRNA) sequencing (277), microRNA sequencing (293), DNA methylation profiling (289), *TERT* promoter sequencing (287), and reverse-phase protein lysate array (RPPA) profiling (255).²² Complete data for all platforms were available for 254 samples. Whole-genome sequencing and low-pass whole-genome sequencing were performed on 21 and 52 samples, respectively. Molecular data were frozen on January 31, 2014, and clinical data were frozen on August 25, 2014. We also performed an unsupervised analysis (i.e., an analysis in which the categories are not known before computation) that integrated results from multiple platforms, including cluster of clusters (CoC) and OncoSign.²³ In brief, CoC is a second-level clustering of class assignments derived from each individual molecular platform. OncoSign classifies tumors on the basis of similarities in recurrent mutations and copy-number variations.

The complete data sets are provided in Table S1 (Supplementary Appendix 2). The primary sequence files are deposited in CGHub (<https://cghub.ucsc.edu>); all other data, including mutation annotation files, are deposited at the Cancer Genome Atlas Data Coordinating Center (<http://cancergenome.nih.gov>). Sample lists, data matrixes, and supporting data are available at the Cancer Genome Atlas lower-grade glioma publication page (https://tcga-data.nci.nih.gov/docs/publications/lgg_2015).

STATISTICAL ANALYSIS

The statistical analysis included Fisher's exact test for associations of categorical variables, one-way analysis of variance for association with continuous outcomes, Kaplan–Meier estimates of survival with log-rank tests among strata, and Cox proportional-hazards regression for multiple-predictor models of survival. A complete description of the methods is provided in Supplementary Appendix 1.

RESULTS

HISTOLOGIC AND MOLECULAR SUBTYPES

To compare the results from molecular platforms with both histologic classification and classification based on markers frequently used in clinical practice (*IDH* mutation and 1p/19q codeletion), we classified lower-grade gliomas into three categories: gliomas with an *IDH* mutation and 1p/19q codeletion, gliomas with an *IDH* mutation and no 1p/19q codeletion, and gliomas with wild-type *IDH*. We found a strong correlation between the presence of an *IDH* mutation and 1p/19q codeletion and the oligodendroglioma histologic class (69 of 84 samples) (Table 1, and Table S2 in Supplementary Appendix 1), a finding consistent with that in previous studies.^{24,25} Glioma samples with an *IDH* mutation and no 1p/19q codeletion (139 samples, 50% of the cohort) represented a mixture of histologic classes but were enriched for astrocytomas and oligoastrocytomas. *IDH* wild-type samples

were mostly astrocytomas (31 of 55 samples) and grade III gliomas (42 of 55 samples), but this group included other histologic classes and grades. Overall, classification based on *IDH*-1p/19q status correlated strongly with the oligodendroglioma histologic class but only modestly with astrocytoma and oligoastrocytoma.

MULTIPLATFORM INTEGRATIVE ANALYSIS

To determine whether advanced molecular profiling could subdivide lower-grade gliomas into discrete sets that are associated with biologic characteristics of disease, we performed unsupervised clustering of molecular data derived from four independent platforms and found well-defined clusters based on DNA methylation (five clusters) (Fig. S1 through S5 in Supplementary Appendix 1), gene expression (four clusters) (Fig. S6 and S7 in Supplementary Appendix 1 and Table S7 [Supplementary Appendix 6]), DNA copy number (three clusters) (Fig. S8 in Supplementary Appendix 1), and microRNA expression (four clusters) (Fig. S9 and S10 in Supplementary Appendix 1 and Table S8 [Supplementary Appendix 7] and Table S9 [Supplementary Appendix 8]).^{22,26,27} To integrate data and compare the resulting biologic classes with histologic classes and subtypes based on *IDH*-1p/19q status, cluster group assignments from the four individual platforms (DNA methylation, mRNA, DNA copy number, and microRNA) were used for a second-level CoC analysis, resulting in three CoC clusters with distinctive biologic themes (Fig. 1). We found a strong correlation between CoC cluster assignment and molecular subtypes defined on the basis of *IDH*-1p/19q codeletion status: most lower-grade gliomas with wild-type *IDH* were in the CoC cluster that included mRNA cluster R2, microRNA cluster Mi3, DNA methylation cluster M4, and DNA copy number cluster C2. Another CoC cluster contained almost all gliomas with an *IDH* mutation and 1p/19q codeletion and included primarily clusters R3, M2 and M3, and C3. The third CoC cluster was highly enriched for gliomas with an *IDH* mutation and no 1p/19q codeletion and included clusters R1, M5, C1, and Mi1.

To determine the relative strength of clinical schemes for the classification of lower-grade gliomas in capturing the biologic subsets revealed by CoC analysis, we compared the correlation between *IDH*-1p/19q subtype and CoC cluster assignment with the correlation between histologic class and CoC cluster assignment. Whereas 90% of samples with a specific *IDH*-1p/19q designation mapped one-to-one with a predominant CoC cluster, only 63% of samples within a specific histologic class showed this predominant mapping. Moreover, the concordance between *IDH*-1p/19q status and CoC cluster assignment was much greater than that between histologic subtype and CoC cluster assignment (adjusted Rand index, 0.79 vs. 0.19) (Table S2E in Supplementary Appendix 1), which indicates that *IDH*-1p/19q status captures the biologic characteristics of lower-grade gliomas with greater fidelity than does histologic class.

MUTATIONAL LANDSCAPE OF LOWER-GRADE GLIOMAS

We generated a consensus mutation set with the use of three mutation-calling algorithms (see the Methods section in Supplementary Appendix 1); this yielded 9885 mutations detected in 289 samples (0.66 mutations per megabase in coding regions; median, 29 mutations per sample [range, 0 to 597]). Samples of lower-grade gliomas with wild-type *IDH* had more mutations (median, 45) than did samples with an *IDH* mutation and 1p/19q

codeletion (median, 27; $P < 0.001$) or those with an *IDH* mutation and no 1p/19q codeletion (median, 28; $P < 0.001$) (Fig. S11, S12, and S13 in Supplementary Appendix 1). The prevalence of mutations in lower-grade gliomas, per individual sample, was lower than that in glioblastoma, higher than that in medulloblastoma, and intermediate in the spectrum of Cancer Genome Atlas–reported cancers (Fig. S11 in Supplementary Appendix 1).^{22,28}

We identified significant differences in DNA copy-number alterations and gene mutations among the three molecular subtypes (Fig. 2, 3, and 4, and Fig. S8 and S14 in Supplementary Appendix 1, Table S3 [Supplementary Appendix 3], and Table S4 in Supplementary Appendix 1). We found *CIC* mutations in 62% and *FUBP1* mutations in 29% of lower-grade gliomas with an *IDH* mutation and 1p/19q codeletion, but we did not find these mutations in the other molecular subtypes. Among lower-grade gliomas with an *IDH* mutation and 1p/19q codeletion, we also observed mutations in the PI3 kinase pathway genes *PIK3CA* (20%) and *PIK3R1* (9%)²⁹ and in *NOTCH1* (31%),^{29–31} as well as novel mutations in *ZBTB20* (9%) and *ARID1A* (6%) (Fig. 2). In addition, among lower-grade gliomas with an *IDH* mutation and 1p/19q codeletion, 96% carried activating *TERT* promoter mutations, leading to elevated *TERT* expression; *ATRX* mutations were rare in these tumors, a finding consistent with the mutual exclusivity of *ATRX* and *TERT* mutations^{14,32} (Fig. 2 and 3). Focal amplification of 19p13.3 was noted (Fig. 3, and Fig. S14A in Supplementary Appendix 1), but few recurring whole-arm copy-number alterations other than 1p/19q codeletion were observed (Fig. S8B in Supplementary Appendix 1). Differences in the prevalence of mutations and the pattern of copy-number alterations between grade II and grade III lower-grade gliomas with an *IDH* mutation and 1p/19q codeletion were modest (Fig. 5A, and Fig. S21 in Supplementary Appendix 1).

Overall, the data suggest that lower-grade gliomas with an *IDH* mutation and 1p/19q codeletion are biologically discrete and arise from a sequence of *IDH* mutation, 1p/19q codeletion, and *TERT* activation; mutation of *CIC* and *FUBP1*; and activating alterations in the PI3 kinase pathway.^{29,31,32} *NOTCH1* mutations in this subset of tumors probably inactivate the gene, because they occur at positions similar to those of *NOTCH1* inactivating mutations in lung, head and neck, and cervical cancers and not at activation sites³⁴ (Fig. S15 in Supplementary Appendix 1). The results of a PARADIGM-SHIFT³⁵ analysis (Fig. S16 in Appendix 1), in which downstream targets are evaluated to assess pathway status, also suggested that *NOTCH1* mutations result in inactivation of NOTCH1 protein function. Previous studies identified *NOTCH1* mutations in oligodendroglioma and anaplastic astrocytoma; we noted them most often in lower-grade gliomas with an *IDH* mutation and 1p/19q codeletion, and they were rarely identified in lower-grade gliomas with an *IDH* mutation and no 1p/19q codeletion or in those with wild-type *IDH* (Fig. 2).^{29–31}

Nearly all lower-grade gliomas with an *IDH* mutation and no 1p/19q codeletion (94%) harbored *TP53* mutations, which suggests that this tumor class is defined by a loss of p53 function. Inactivating alterations of *ATRX* were frequent (86%) and included mutations (79%), deletions (3%), gene fusion (2%), or a combination of these events (2%).¹⁹ *TERT* promoter mutations were rare (4%), a finding consistent with the alternative mechanism of lengthening telomeres that is associated with *ATRX* mutations.³² We observed two novel significantly mutated genes in lower-grade gliomas with an *IDH* mutation and no 1p/19q

codeletion: the SWI/SNF chromatin remodeler *SMARCA4* (in 6% of these gliomas), which was previously implicated in glioma progression,³⁶ and the translation initiation factor *EIF1AX* (in <1%), which was previously documented in uveal melanoma³⁷ (Fig. 2, and Table S4 in Supplementary Appendix 1). Some lower-grade gliomas with an *IDH* mutation and no 1p/19q codeletion had focal gains of 4q12, a locus harboring *PDGFRA*, which encodes a receptor tyrosine kinase; 12q14, encompassing *CDK4*, which encodes a cell-cycle regulator; or 8q24, a broad amplicon that includes *MYC* (Fig. S14A in Supplementary Appendix 1). These findings are consonant with those in previous studies of proneural glioblastoma with mutated *IDH1* (with respect to *MYC* amplification) and with wild-type *IDH1* (with regard to *CDK4* and *PDGFRA* amplification).²² Histologic grade III tumors in this subset had greater frequencies of chromosome 9p and 19q losses and of 10p gains (Fig. 5A), yet the mutational profiles did not differ substantially between grades (Fig. S21B in Supplementary Appendix 1). In the class of lower-grade gliomas with an *IDH* mutation, our multiplatform analysis suggests that there is a molecular progression that starts with initial *IDH* mutation and acquisition of the glioma CpG island methylation phenotype (G-CIMP, a specific pattern of widespread DNA hypermethylation) and is followed by either 1p/19q codeletion or *TP53* mutation.^{19,31,38}

SIGNALING NETWORKS IN LOWER-GRADE GLIOMA

To incorporate mutational landscapes into an unsupervised multiplatform classification, we performed OncoSign analysis²³ with the use of 70 selected genetic events (mutation and copy number alteration) and identified four dominant subtypes (OSC1 to OSC4), which again largely recapitulated those defined by *IDH*-1p/19q status (adjusted Rand index, 0.83) (Fig. 3, and Table S2E in Supplementary Appendix 1). OSC1 was strongly correlated with lower-grade gliomas with an *IDH* mutation and no 1p/19q codeletion, and OSC4 contained exclusively lower-grade gliomas with wild-type *IDH*. The group with an *IDH* mutation and 1p/19q codeletion included both OSC2 and OSC3 lower-grade gliomas, which differed from one another with regard to mutations in *CIC*, *FUBP1*, and *NOTCH1* yet were not substantially different in terms of tumor grade or patient outcome. The concordance between *IDH*-1p/19q status and classes based on two different multiplatform approaches to genomic data integration (CoC and OncoSign) is striking and contrasts sharply with the much weaker correlation between histologic subtypes and unsupervised multiplatform classes (Table S2E in Supplementary Appendix 1). The finding that widely available markers (*IDH* and 1p/19q) can be used to classify lower-grade gliomas with results similar to those obtained through the unsupervised stratification of genomewide molecular data provides an unbiased, data-driven rationale for using *IDH* and 1p/19q markers to identify lower-grade glioma disease classes and to incorporate them into a contemporary clinical classifier.^{11,14,39,40}

LOWER-GRADE GLIOMAS AND GLIOBLASTOMA WITH WILD-TYPE *IDH*

Mutations in seven genes were strongly associated with lower-grade gliomas that had wild-type *IDH*. Five of these genes have been reported to be mutated in glioblastoma: *PTEN* (in 23% of lower-grade gliomas with wild-type *IDH*), *EGFR* (in 27%), *NF1* (in 20%), *TP53* (in 14%), and *PIK3CA* (in 9%).²² We also found novel mutations in *PTPN11*, which encodes protein tyrosine phosphatase non-receptor 11 (in 7%), and in *PLCG1*, which encodes phospholipase C gamma 1 (in 5%) (Fig. 2). Similarly, copy-number alterations in tumors

with wild-type *IDH* were distinct from lower-grade gliomas with mutated *IDH* and instead resembled glioblastomas with wild-type *IDH* (Fig. 5A). In particular, gains of chromosome 7 and deletions of chromosome 10 co-occurred in more than 50% of tumors of this subtype (chromosome 7 gains, 56%; chromosome 10 deletions, 63%), yet these alterations were absent in groups with mutated *IDH*. Recurring focal amplifications containing *EGFR*, *MDM4*, and *CDK4* (in 38%, 13%, and 7% of tumors, respectively) and focal deletions targeting *CDKN2A* and *RBI* (in 63% and 25%, respectively) were the most common acquired copy-number variants in lower-grade gliomas with wild-type *IDH*, findings similar to those for glioblastomas with wild-type *IDH* (Fig. 5B). Grade II gliomas with wild-type *IDH* were uncommon (13 cases), yet they differed from those that were grade III (Fig. S21C and S21D in Supplementary Appendix 1) in that they were strongly enriched within the discrete M1 DNA methylation cluster (Fig. 1, and Fig. S1A in Supplementary Appendix 1). Lower-grade gliomas in the M1 cluster that had wild-type *IDH* and were of grade II had a low prevalence of mutations and copy-number alterations, and they did not have *TERT* promoter mutations, which potentially indicates that they are distinct pathologic entities. *TERT* promoter mutations were present in 64% of all lower-grade gliomas with wild-type *IDH*; when M1 lower-grade gliomas were excluded from the analysis, *TERT* promoter mutations were present in 80% of those remaining, a prevalence similar to that in primary glioblastoma.³²

GENOMIC REARRANGEMENTS AND FUSION TRANSCRIPTS

We investigated 20 samples with the use of high-coverage whole-genome sequencing, 50 samples with low-coverage whole-genome sequencing, and 311 samples with whole-exome sequencing, for structural chromosomal variants (e.g., translocations and inversions); we uncovered, with high confidence, 250 chromosomal rearrangements (Table S5 [Supplementary Appendix 4]). In addition, 19 samples had evidence of extra-chromosomal DNA structures known as double-minute chromosomes–breakpoint-enriched regions (DM-BERs) (Table S5 [Supplementary Appendix 4] and Fig. S17 in Supplementary Appendix 1). Of these, 15 occurred in lower-grade gliomas with wild-type *IDH* (27% of the samples) (Fig. 5A), a frequency similar to that seen with glioblastoma (23%).^{41,42} In an analysis of RNA sequencing data, we identified fusion transcripts in 265 lower-grade gliomas (Table S6 [Supplementary Appendix 5]), and correlation with structural genomic variants suggested chimeric transcription for 44% of the high-confidence chromosomal rearrangements, including two *EGFR* fusions (Fig. 5B), and for 58% of DM-BERs.^{43,44} Several genes (*EGFR*, *FGFR3*, *NOTCH1*, *ATRX*, and *CDK4*) were affected by fusions in multiple samples (Fig. S18A and S18B in Supplementary Appendix 1). Fusions that were predicted to activate *EGFR* and *FGFR3* were restricted to lower-grade gliomas with wild-type *IDH* and were noted at frequencies similar to those in glioblastoma (7% and 3%, respectively) (Fig. S18A, S18B, and S19 in Supplementary Appendix 1).^{45,46} A novel chimeric *FGFR3-ELAVL3* transcript involved the same breakpoint as previously reported for *FGFR3-TACC3* fusions and was highly expressed, which suggests that it could have similar effects on *FGFR3* function. Three samples had fusions between *EGFR* and intergenic or intronic chromosome 7 regions that are predicted to remove the EGFR autophosphorylation domain and are likely to be oncogenic (Fig. S18 in Supplementary Appendix 1).⁴⁷ Fusions involving genes encoding receptor tyrosine kinases were predominantly a feature of lower-grade gliomas

with wild-type *IDH*; only two lower-grade gliomas with an *IDH* mutation and no 1p/19q codeletion harbored such fusions (involving *PDGFRA* and *MET*), and none were identified among lower-grade gliomas with an *IDH* mutation and 1p/19q codeletion.

PROTEIN EXPRESSION

RPPA analysis resulted in protein-expression profiles that showed a striking segregation of lower-grade gliomas with wild-type *IDH* from those with mutated *IDH*, as well as the activation of receptor tyrosine kinase pathways (such as the EGFR pathway) in tumors with wild-type *IDH*, which provides additional support for the biologic similarity between lower-grade gliomas with wild-type *IDH* and glioblastoma (Fig. S20 in Supplementary Appendix 1). We observed over-expression of HER2, a potential therapeutic target, in tumors with wild-type *IDH*. Among lower-grade gliomas with mutated *IDH*, we observed higher expression of tyrosine protein kinase SYK, E-cadherin, and annexin 1 in the group without 1p/19q codeletion. Among lower-grade gliomas with an *IDH* mutation and 1p/19q codeletion, we noted higher levels of HER3 with a phosphorylated tyrosine residue at position 1289, a marker that potentially confers resistance to PI3 kinase inhibitors.⁴⁸

FROM SIGNATURES TO PATHWAYS

To gain insights into signaling pathways, we performed an integrated analysis of mutations, focal copy-number alterations, structural variants, and fusions affecting genes that encode receptor tyrosine kinases (*EGFR*, *PDGFRA*, *MET*, and *FGFR*), PI3 kinase subunits, MAP kinases *NF1* and *BRAF*, components of the p53 and RB1 pathways (*MDM2*, *MDM4*, *MDM1*, *CDKN2A* and *CDKN2B* [hereafter referred to as *CDKN2A/B*], and *CDKN2C*), and *ATRX*. Alterations across these loci were remarkably similar in frequency between lower-grade gliomas with wild-type *IDH* and glioblastomas with wild-type *IDH* but not between these groups and other subtypes of lower-grade glioma (Fig. 5B, and Fig. S21E in Supplementary Appendix 1).²² A total of 43% of lower-grade gliomas with wild-type *IDH* and 53% of glioblastomas with wild-type *IDH* harbored *EGFR* alterations, with *EGFR* amplification being the most common aberration in both (Fig. S21 in Supplementary Appendix 1). Homozygous *CDKN2A/B* deletions occurred in 45% of lower-grade gliomas with wild-type *IDH*, which is similar to the frequency of these deletions in glioblastomas with wild-type *IDH* (55%). This contrasts with lower-grade gliomas with an *IDH* mutation and no 1p/19q codeletion, in which large single-copy deletions of chromosome 9p were common, yet *CDKN2A/B* was homozygously deleted in only 4% (Fig. S14B in Supplementary Appendix 1). Lower-grade gliomas with mutated *IDH* did not have cancer pathway aberrations similar to those of glioblastoma with wild-type *IDH*; instead, they had characteristic cancer pathway alterations in *TP53* and *ATRX* (in the group with *IDH* mutation and no 1p/19q codeletion) and in *TERT*, *NOTCH1*, *CIC*, and *FUBP1* (in the group with *IDH* mutation and 1p/19q codeletion) (Fig. S21E in Supplementary Appendix 1).

CLINICAL CHARACTERISTICS AND OUTCOMES ASSOCIATED WITH MOLECULAR SUBTYPES

Patients who had lower-grade gliomas with wild-type *IDH* were older than those who had lower-grade gliomas with mutated *IDH* and were more likely to have a family history of

cancer (Table 1, and Table S2 in Supplementary Appendix 1). The anatomical locations of the tumors also differed; lower-grade gliomas with mutated *IDH* arose in frontal lobes more often than did those with wild-type *IDH* ($P < 0.05$). Among the patients for whom clinical follow-up data were available, 77 of 250 (31%) had tumor recurrence, and 60 of 289 (21%) were deceased at the time of analysis. Patients who had lower-grade gliomas with wild-type *IDH* had substantially shorter overall survival than did those with lower-grade gliomas with mutated *IDH* (age-adjusted hazard ratio for death, 7.4; 95% confidence interval, 4.0 to 13.8). Their prognosis (median survival, 1.7 years) was intermediate between those of persons who had glioblastomas with wild-type *IDH* (median survival, 1.1 years) and persons who had glioblastomas with mutated *IDH* (median survival, 2.1 years) (Fig. 6B, and Table S2D in Supplementary Appendix 1). In comparison, persons who had lower-grade gliomas with an *IDH* mutation and 1p/19q codeletion had a median survival of 8.0 years, and those with an *IDH* mutation and no codeletion had a median survival of 6.3 years.

The molecular classification of lower-grade gliomas as having wild-type *IDH*, *IDH* mutation with no 1p/19q codeletion, or *IDH* mutation with 1p/19q codeletion stratified patient outcomes in multiple-predictor models after adjustment for age and extent of resection (Table S2B, S2C, and S2D in Supplementary Appendix 1). Grade, but not histologic class, remained a significant predictor of outcome in multivariable models with *IDH*–1p/19q status and provided additional prognostic value among the molecular subsets (Table S2 and Fig. S22 in Supplementary Appendix 1). Together, the results point to three robust tumor classes in lower-grade glioma, each with prototypical molecular alterations and distinctive clinical behavior (Fig. 4 and 6B).

DISCUSSION

We used a comprehensive, multiplatform genomics approach to delineate the biologic foundations of adult lower-grade glioma and conclude that genetic status was more reflective of disease subtypes than was histologic class. We base this conclusion on the results of an unsupervised analysis of genomewide molecular platforms, in which we identified three cohesive tumor classes that had distinct clinical behavior and were concordant with *IDH*, 1p/19q, and *TP53* status to a greater extent than with histologic class. The three nonoverlapping molecular subtypes distilled from the six histologic and grade combinations lay the foundation for a reproducible and clinically relevant classification that incorporates molecular data into the pathological diagnosis, as is planned for the upcoming revision of the WHO classification of brain tumors.^{39,40} More specifically, we observed that two unsupervised, integrative genomewide analyses independently uncovered three primary lower-grade glioma disease classes that were best represented by *IDH* and 1p/19q status; that lower-grade gliomas with an *IDH* mutation had either 1p/19q codeletion or a *TP53* mutation in a mutually exclusive fashion, which indicates a strict molecular dichotomy; and that the majority of lower-grade gliomas with wild-type *IDH* showed remarkable genomic and clinical similarity to primary (wild-type *IDH*) glioblastoma.

Numerous studies have shown that the histopathological classification of diffuse gliomas is prone to high interobserver variation, correlates inconsistently with genetic markers, and imperfectly predicts clinical outcomes.^{9,10} Like others, we found that lower-grade gliomas

with an *IDH* mutation and 1p/19q codeletion were of the oligodendroglioma histologic class and were associated with favorable outcomes.^{1,4,14,18,24,49} However, lower-grade gliomas with wild-type *IDH* and those with mutated *IDH* and no 1p/19q codeletion had substantial representation from all three histologic classes (astrocytoma, oligodendroglioma, and oligoastrocytoma), which highlights the discordance between histologic and genetic markers. In comparison, two unsupervised methods that integrated multiplatform molecular data (CoC and OncoSign) yielded strong correlations with *IDH*–1p/19q status (adjusted Rand index, 0.79 and 0.83, respectively), which showed that molecular classification captured biologic classes of disease more accurately than did histologic classification.

In addition, whereas oligodendrogliomas typically had 1p/19q codeletion and astrocytomas typically did not, oligoastrocytomas were distributed among the three molecular subtypes with no molecular feature distinguishing them. Thus, although previous WHO classifications have recognized lower-grade gliomas with mixed histologic features (oligoastrocytoma), our results indicate that lower-grade gliomas with an *IDH* mutation have either 1p/19q codeletion or a *TP53* mutation, with few gaps or overlaps, reflecting two distinct molecular mechanisms of oncogenesis, and they do not provide evidence for a biologic or genetic signature specific to oligoastrocytoma (Fig. 2, 3, and 4); this observation is consistent with those in previous studies.^{38,49–51} Molecular signatures of lower-grade glioma lend themselves to a practice-altering, biologically based classification system that should improve interobserver concordance. The implementation of this type of system also seems likely to reduce the diagnosis of “oligoastrocytoma” and the confusion related to its clinical management.

Another substantial finding was that tumors with wild-type *IDH* were molecularly and clinically distinct from subtypes with mutated *IDH*, with most showing a striking resemblance to primary glioblastoma on all analytic platforms. These findings suggest that lower-grade gliomas with wild-type *IDH* are likely to be immediate precursors of glioblastoma with wild-type *IDH*, since the median survival associated with this type of lower-grade glioma was only slightly longer than that associated with this type of glioblastoma (Fig. 6B). Alternatively, such tumors could represent glioblastomas that were incompletely sampled during surgery, in which case definitive histologic classification would be precluded. From a practical standpoint, sampling errors represent a challenge in surgical neuropathology, regardless of *IDH* status, class, or grade, because a histologic diagnosis is limited to findings under the microscope. Thus, molecular classification based on *IDH*–1p/19q status represents an improvement in diagnostic practice because it enables the identification of a clinically aggressive form of lower-grade glioma (with wild-type *IDH*) in the absence of morphologic criteria for glioblastoma.^{15,17}

Our analysis of clinical outcomes showed that persons who had lower-grade gliomas with an *IDH* mutation and no 1p/19q codeletion had shorter overall survival than did those who had lower-grade gliomas with an *IDH* mutation with codeletion, yet both of these groups had substantially longer overall survival than did persons who had lower-grade gliomas with wild-type *IDH*.¹⁵ The stratification of clinical risk on the basis of *IDH*–1p/19q status is more robust than outcome predictions based on histologic class (Fig. 6, and Table S2 and Fig. S22 in Supplementary Appendix 1). Molecular classification can also provide quality control for

histopathological diagnosis. For example, tumors in the small, discrete DNA methylation cluster M1 had a low frequency of mutations and copy-number alterations, yet tumors in this group occasionally contained *BRAF* alterations. Although they are not entirely specific, these alterations are more characteristic of grade I circumscribed tumors, such as pilocytic astrocytoma and ganglioglioma, and their presence would prompt consideration of alternative diagnoses.^{1,13} Although diffuse gliomas and circumscribed gliomas can occasionally overlap histologically, their associated prognosis and clinical management differ greatly. Molecular signatures offer the potential to resolve these diagnostically challenging cases.¹⁴ Further analysis of survival data in our cohort as it matures will be required to improve risk stratification with the use of molecular markers. In addition, ongoing acquisition and maturation of detailed data on treatment and outcomes will aid in the delineation of markers that are predictive of therapeutic response. In the meantime, however, the use of molecular classification can be integrated with other clinical, neuroimaging, and pathological data to devise a treatment strategy for individual patients.

It may transpire that distinct therapeutic strategies are required for effective disease control in molecular subtypes of lower-grade glioma. Molecular inclusion criteria and stratification in clinical-trial design will be necessary for a clear interpretation of outcomes from specific treatments. The prevalence of *IDH* mutations in lower-grade glioma invites targeting of either the mutant enzymes themselves or their downstream metabolic and epigenomic consequences, such as G-CIMP.⁵² Mutations in *ATRX*, *CIC*, and *FUBP1* have only recently been implicated in cancer pathogenesis, yet their specificity and prevalence in lower-grade glioma with an *IDH* mutation support central roles in oncogenesis and argue for thorough characterization of associated signaling networks to facilitate therapeutic development. The genetic and clinical similarities between lower-grade glioma with wild-type *IDH* and primary glioblastoma support the potential inclusion of this type of lower-grade glioma within the broad spectrum of glioblastoma-related clinical investigation and treatment protocols. Finally, our integrative analysis has shown that all subtypes of lower-grade glioma rely to some extent on core signaling networks that have previously been implicated in glioblastoma pathogenesis, many of which are targeted by agents that are being evaluated in clinical trials.

Supplementary Material

Refer to Web version on PubMed Central for supplementary material.

Acknowledgments

Supported by grants (U24CA143883, U24CA143858, U24CA143840, U24CA143799, U24CA143835, U24CA143845, U24CA143882, U24CA143867, U24CA143866, U24CA143848, U24CA144025, U54HG003067, U54HG003079, U54HG003273, U24CA126543, U24CA126544, U24CA126546, U24CA126551, U24CA126554, U24CA126561, U24CA126563, U24CA143731, U24CA143843, and P30CA016672) from the National Institutes of Health.

We thank personnel at the genome sequencing centers and cancer genome characterization centers for data generation and analyses, members of the National Cancer Institute and National Human Genome Research Institute project teams for coordination of project activities, and personnel at the M.D. Anderson Functional Proteomics Core for RPPA data and analysis.

Glossary

Adjusted Rand index	A measure of the similarity between two data clusterings, adjusted for chance grouping of the elements
Cluster of clusters (CoC) analysis	A method of obtaining clusters (e.g., of patient samples) that represent a consensus among the individual data types (in this study, we incorporated DNA methylation, DNA copy number, mRNA expression, and microRNA expression into the analysis)
Double-minute chromosome–breakpoint-enriched region (DM-BER)	As detected by whole-exome and whole-genome sequencing, highly amplified gene regions that are connected by DNA rearrangement breakpoints and allow cancer cells to maintain high levels of oncogene amplification
Exon	The portion of a gene that encodes amino acids to form a protein
Fusion transcript	A transcript composed of parts of two separate genes joined together by a chromosomal rearrangement, in some cases with functional consequences for oncogenesis, therapy, or both
Glioblastoma	The highest-grade (World Health Organization grade IV) and most frequently occurring form of diffusely infiltrative astrocytoma. It arises most often in the cerebral hemispheres of adults and is distinguished histopathologically from diffuse lower-grade astrocytomas (grades II and III) by the presence of necrosis or microvascular proliferation
Lower-grade glioma	A diffusely infiltrative low-grade or intermediate-grade glioma (World Health Organization grade II or III) that arises most often in the cerebral hemispheres of adults and includes astrocytomas, oligodendrogliomas, and oligoastrocytomas
Methylation	The attachment of methyl groups to DNA at cytosine bases. Methylation is correlated with reduced transcription of the gene immediately downstream of the methylated site
microRNA	A short regulatory form of RNA that binds to a target RNA and generally suppresses its translation by ribosomes
Molecular subtype	Subgroup of a tumor type based on molecular characteristics (rather than, e.g., histologic or clinical features); in this study, a molecular subtype is one of three classes based on <i>IDH</i> mutation and 1p/19q codeletion status
Mutation frequency	The number of mutations detected per megabase of DNA

Significantly mutated gene	A gene with a greater number of mutations than expected on the basis of the background mutation rate, which suggests a role in oncogenesis
Whole-exome sequencing	Sequencing of the coding regions, or exons, of an entire genome
Whole-genome sequencing	Sequencing of the entire genome

References

1. Louis, DN.; Ohgaki, H.; Wiestler, OD.; Cavenee, WK. WHO classification of tumours of the central nervous system. 4. Lyon, France: International Agency for Research; 2007.
2. Ostrom QT, Gittleman H, Farah P, et al. CBTRUS statistical report: Primary brain and central nervous system tumors diagnosed in the United States in 2006–2010. *Neuro Oncol.* 2013; 15(Suppl 2):iii1–ii56. [PubMed: 24137015]
3. Macdonald DR, Gaspar LE, Cairn-cross JG. Successful chemotherapy for newly diagnosed aggressive oligodendroglioma. *Ann Neurol.* 1990; 27:573–4. [PubMed: 2360797]
4. van den Bent MJ. Practice changing mature results of RTOG study 9802: another positive PCV trial makes adjuvant chemotherapy part of standard of care in low-grade glioma. *Neuro Oncol.* 2014; 16:1570–4. [PubMed: 25355680]
5. van den Bent MJ, Brandes AA, Taphoorn MJ, et al. Adjuvant procarbazine, lomustine, and vincristine chemotherapy in newly diagnosed anaplastic oligodendroglioma: long-term follow-up of EORTC brain tumor group study 26951. *J Clin Oncol.* 2013; 31:344–50. [PubMed: 23071237]
6. Bourne TD, Schiff D. Update on molecular findings, management and outcome in low-grade gliomas. *Nat Rev Neurol.* 2010; 6:695–701. [PubMed: 21045797]
7. Sanai N, Chang S, Berger MS. Low-grade gliomas in adults. *J Neurosurg.* 2011; 115:948–65. [PubMed: 22043865]
8. Jakola AS, Myrnel KS, Kloster R, et al. Comparison of a strategy favoring early surgical resection vs a strategy favoring watchful waiting in low-grade gliomas. *JAMA.* 2012; 308:1881–8. [PubMed: 23099483]
9. Coons SW, Johnson PC, Scheithauer BW, Yates AJ, Pearl DK. Improving diagnostic accuracy and interobserver concordance in the classification and grading of primary gliomas. *Cancer.* 1997; 79:1381–93. [PubMed: 9083161]
10. van den Bent MJ. Interobserver variation of the histopathological diagnosis in clinical trials on glioma: a clinician’s perspective. *Acta Neuropathol.* 2010; 120:297–304. [PubMed: 20644945]
11. Theeler BJ, Yung WK, Fuller GN, De Groot JF. Moving toward molecular classification of diffuse gliomas in adults. *Neurology.* 2012; 79:1917–26. [PubMed: 23109653]
12. Weller M, Stupp R, Hegi ME, et al. Personalized care in neurooncology coming of age: why we need MGMT and 1p/19q testing for malignant glioma patients in clinical practice. *Neuro Oncol.* 2012; 14(Suppl 4):iv100–iv108. [PubMed: 23095825]
13. Appin CL, Brat DJ. Molecular genetics of gliomas. *Cancer J.* 2014; 20:66–72. [PubMed: 24445767]
14. Eckel-Passow JE, Lachance DH, Molinaro AM, et al. Glioma groups based on 1p/19q, *IDH*, and *TERT* promoter mutations in tumors. *N Engl J Med.* 2015; 372:2499–508. [PubMed: 26061753]
15. Jiao Y, Killela PJ, Reitman ZJ, et al. Frequent ATRX, CIC, FUBP1 and IDH1 mutations refine the classification of malignant gliomas. *Oncotarget.* 2012; 3:709–22. [PubMed: 22869205]
16. Parsons DW, Jones S, Zhang X, et al. An integrated genomic analysis of human glioblastoma multiforme. *Science.* 2008; 321:1807–12. [PubMed: 18772396]
17. Yan H, Parsons DW, Jin G, et al. IDH1 and IDH2 mutations in gliomas. *N Engl J Med.* 2009; 360:765–73. [PubMed: 19228619]

18. Cairncross G, Wang M, Shaw E, et al. Phase III trial of chemoradiotherapy for anaplastic oligodendroglioma: long-term results of RTOG 9402. *J Clin Oncol.* 2013; 31:337–43. [PubMed: 23071247]
19. Liu XY, Gerges N, Korshunov A, et al. Frequent ATRX mutations and loss of expression in adult diffuse astrocytic tumors carrying IDH1/IDH2 and TP53 mutations. *Acta Neuropathol.* 2012; 124:615–25. [PubMed: 22886134]
20. Zhang J, Wu G, Miller CP, et al. Whole-genome sequencing identifies genetic alterations in pediatric low-grade gliomas. *Nat Genet.* 2013; 45:602–12. [PubMed: 23583981]
21. Rodriguez FJ, Tihan T, Lin D, et al. Clinicopathologic features of pediatric oligodendrogliomas: a series of 50 patients. *Am J Surg Pathol.* 2014; 38:1058–70. [PubMed: 24805856]
22. Brennan CW, Verhaak RG, McKenna A, et al. The somatic genomic landscape of glioblastoma. *Cell.* 2013; 155:462–77. [PubMed: 24120142]
23. Ciriello G, Miller ML, Aksoy BA, Senbabaoglu Y, Schultz N, Sander C. Emerging landscape of oncogenic signatures across human cancers. *Nat Genet.* 2013; 45:1127–33. [PubMed: 24071851]
24. Aldape K, Burger PC, Perry A. Clinicopathologic aspects of 1p/19q loss and the diagnosis of oligodendroglioma. *Arch Pathol Lab Med.* 2007; 131:242–51. [PubMed: 17284109]
25. Giannini C, Burger PC, Berkey BA, et al. Anaplastic oligodendroglial tumors: refining the correlation among histopathology, 1p 19q deletion and clinical outcome in Intergroup Radiation Therapy Oncology Group Trial 9402. *Brain Pathol.* 2008; 18:360–9. [PubMed: 18371182]
26. Noushmehr H, Weisenberger DJ, Diefes K, et al. Identification of a CpG island methylator phenotype that defines a distinct subgroup of glioma. *Cancer Cell.* 2010; 17:510–22. [PubMed: 20399149]
27. Verhaak RG, Hoadley KA, Purdom E, et al. Integrated genomic analysis identifies clinically relevant subtypes of glioblastoma characterized by abnormalities in PDGFRA, IDH1, EGFR, and NF1. *Cancer Cell.* 2010; 17:98–110. [PubMed: 20129251]
28. Lawrence MS, Stojanov P, Polak P, et al. Mutational heterogeneity in cancer and the search for new cancer-associated genes. *Nature.* 2013; 499:214–8. [PubMed: 23770567]
29. Bettegowda C, Agrawal N, Jiao Y, et al. Mutations in CIC and FUBP1 contribute to human oligodendroglioma. *Science.* 2011; 333:1453–5. [PubMed: 21817013]
30. Killela PJ, Pirozzi CJ, Reitman ZJ, et al. The genetic landscape of anaplastic astrocytoma. *Oncotarget.* 2014; 5:1452–7. [PubMed: 24140581]
31. Yip S, Butterfield YS, Morozova O, et al. Concurrent CIC mutations, IDH mutations, and 1p/19q loss distinguish oligodendrogliomas from other cancers. *J Pathol.* 2012; 226:7–16. [PubMed: 22072542]
32. Killela PJ, Reitman ZJ, Jiao Y, et al. TERT promoter mutations occur frequently in gliomas and a subset of tumors derived from cells with low rates of self-renewal. *Proc Natl Acad Sci U S A.* 2013; 110:6021–6. [PubMed: 23530248]
33. Goldman M, Craft B, Swatloski T, et al. The UCSC Cancer Genomics Browser: update 2013. *Nucleic Acids Res.* 2013; 41:D949–D954. [PubMed: 23109555]
34. Weng AP, Ferrando AA, Lee W, et al. Activating mutations of NOTCH1 in human T cell acute lymphoblastic leukemia. *Science.* 2004; 306:269–71. [PubMed: 15472075]
35. Ng S, Collisson EA, Sokolov A, et al. PARADIGM-SHIFT predicts the function of mutations in multiple cancers using pathway impact analysis. *Bioinformatics.* 2012; 28:i640–6. [PubMed: 22962493]
36. Johnson BE, Mazar T, Hong C, et al. Mutational analysis reveals the origin and therapy-driven evolution of recurrent glioma. *Science.* 2014; 343:189–93. [PubMed: 24336570]
37. Martin M, Maßhöfer L, Temming P, et al. Exome sequencing identifies recurrent somatic mutations in EIF1AX and SF3B1 in uveal melanoma with disomy 3. *Nat Genet.* 2013; 45:933–6. [PubMed: 23793026]
38. Cryan JB, Haidar S, Ramkissoon LA, et al. Clinical multiplexed exome sequencing distinguishes adult oligodendroglial neoplasms from astrocytic and mixed lineage gliomas. *Oncotarget.* 2014; 5:8083–92. [PubMed: 25257301]

39. Louis DN, Perry A, Burger P, et al. International Society Of Neuropathology — Haarlem consensus guidelines for nervous system tumor classification and grading. *Brain Pathol.* 2014; 24:429–35. [PubMed: 24990071]
40. Reuss DE, Sahm F, Schrimpf D, et al. ATRX and IDH1-R132H immunohistochemistry with subsequent copy number analysis and IDH sequencing as a basis for an “integrated” diagnostic approach for adult astrocytoma, oligodendroglioma and glioblastoma. *Acta Neuropathol.* 2015; 129:133–46. [PubMed: 25427834]
41. Sanborn JZ, Salama SR, Grifford M, et al. Double minute chromosomes in glioblastoma multiforme are revealed by precise reconstruction of oncogenic amplicons. *Cancer Res.* 2013; 73:6036–45. [PubMed: 23940299]
42. Zheng S, Fu J, Vegesna R, et al. A survey of intragenic breakpoints in glioblastoma identifies a distinct subset associated with poor survival. *Genes Dev.* 2013; 27:1462–72. [PubMed: 23796897]
43. Torres-García W, Zheng S, Sivachenko A, et al. PRADA: pipeline for RNA sequencing data analysis. *Bioinformatics.* 2014; 30:2224–6. [PubMed: 24695405]
44. McPherson A, Hormozdiari F, Zayed A, et al. deFuse: an algorithm for gene fusion discovery in tumor RNA-Seq data. *PLoS Comput Biol.* 2011; 7(5):e1001138. [PubMed: 21625565]
45. Singh D, Chan JM, Zoppoli P, et al. Transforming fusions of FGFR and TACC genes in human glioblastoma. *Science.* 2012; 337:1231–5. [PubMed: 22837387]
46. Parker BC, Annala MJ, Cogdell DE, et al. The tumorigenic FGFR3-TACC3 gene fusion escapes miR-99a regulation in glioblastoma. *J Clin Invest.* 2013; 123:855–65. [PubMed: 23298836]
47. Cho J, Pastorino S, Zeng Q, et al. Glioblastoma-derived epidermal growth factor receptor carboxyl-terminal deletion mutants are transforming and are sensitive to EGFR-directed therapies. *Cancer Res.* 2011; 71:7587–96. [PubMed: 22001862]
48. Gala K, Chandarlapaty S. Molecular pathways: HER3 targeted therapy. *Clin Cancer Res.* 2014; 20:1410–6. [PubMed: 24520092]
49. Suzuki H, Aoki K, Chiba K, et al. Mutational landscape and clonal architecture in grade II and III gliomas. *Nat Genet.* 2015; 47:458–68. [PubMed: 25848751]
50. Wiestler B, Capper D, Sill M, et al. Integrated DNA methylation and copy-number profiling identify three clinically and biologically relevant groups of anaplastic glioma. *Acta Neuropathol.* 2014; 128:561–71. [PubMed: 25008768]
51. Sahm F, Reuss D, Koelsche C, et al. Farewell to oligoastrocytoma: in situ molecular genetics favor classification as either oligodendroglioma or astrocytoma. *Acta Neuropathol.* 2014; 128:551–9. [PubMed: 25143301]
52. Rohle D, Popovici-Muller J, Palaskas N, et al. An inhibitor of mutant IDH1 delays growth and promotes differentiation of glioma cells. *Science.* 2013; 340:626–30. [PubMed: 23558169]

APPENDIX

The authors’ full names and academic degrees are as follows: Daniel J. Brat, M.D., Ph.D., Roel G.W. Verhaak, Ph.D., Kenneth D. Aldape, M.D., W.K. Alfred Yung, M.D., Sofie R. Salama, Ph.D., Lee A.D. Cooper, Ph.D., Esther Rheinbay, Ph.D., C. Ryan Miller, M.D., Ph.D., Mark Vitucci, Ph.D., Olena Morozova, Ph.D., A. Gordon Robertson, Ph.D., Houtan Noushmehr, Ph.D., Peter W. Laird, Ph.D., Andrew D. Cherniack, Ph.D., Rehan Akbani, Ph.D., Jason T. Huse, M.D., Ph.D., Giovanni Ciriello, Ph.D., Laila M. Poisson, Ph.D., Jill S. Barnholtz-Sloan, Ph.D., Mitchel S. Berger, M.D., Cameron Brennan, M.D., Rivka R. Colen, M.D., Howard Colman, M.D., Ph.D., Adam E. Flanders, M.D., Caterina Giannini, M.D., Ph.D., Mia Grifford, Ph.D., Antonio Iavarone, M.D., Rajan Jain, M.D., Isaac Joseph, B.S., Jaegil Kim, Ph.D., Katayoon Kasaian, B.S., Tom Mikkelsen, M.D., Bradley A. Murray, B.S., Brian Patrick O’Neill, M.D., Lior Pachter, Ph.D., Donald W. Parsons, M.D., Ph.D., Carrie Sougnez, B.S., Erik P. Sulman, M.D., Ph.D., Scott R. Vandenberg, M.D., Ph.D., Erwin G. Van Meir, Ph.D., Andreas von Deimling, M.D., Hailei Zhang, Ph.D., Daniel Crain,

M.B.A., Kevin Lau, B.S., David Mallery, M.B.A., J.D., Scott Morris, P.S.M., Ph.D., Joseph Paulauskis, Ph.D., Robert Penny, M.D., Ph.D., Troy Shelton, M.S., P.M.P., Mark Sherman, Ph.D., Peggy Yena, B.S., Aaron Black, B.S., Jay Bowen, M.S., Katie Dicostanzo, B.S., Julie Gastier-Foster, Ph.D., Kristen M. Leraas, M.S., Tara M. Lichtenberg, B.A., Christopher R. Pierson, M.D., Ph.D., Nilsa C. Ramirez, M.D., Cynthia Taylor, B.S., Stephanie Weaver, Lisa Wise, Erik Zmuda, Ph.D., Tanja Davidsen, Ph.D., John A. Demchok, M.S., Greg Eley, Ph.D., Martin L. Ferguson, Ph.D., Carolyn M. Hutter, Ph.D., Kenna R. Mills Shaw, Ph.D., Bradley A. Ozenberger, Ph.D., Margi Sheth, B.S., Heidi J. Sofia, Ph.D., Roy Tarnuzzer, Ph.D., Zhining Wang, Ph.D., Liming Yang, Ph.D., Jean Claude Zenklusen, Ph.D., Brenda Ayala, B.S., Julien Baboud, B.S., Sudha Chudamani, M.Phil., Mark A. Jensen, Ph.D., Jia Liu, Ph.D., Todd Pihl, Ph.D., Rohini Raman, B.S., Yunhu Wan, Ph.D., Ye Wu, Ph.D., Adrian Ally, B.S., J. Todd Auman, Ph.D., Miruna Balasundaram, B.S., Saianand Balu, M.S., Stephen B. Baylin, M.D., Rameen Beroukhim, M.D., Ph.D., Moiz S. Bootwalla, M.S., Reanne Bowlby, M.S., Christopher A. Bristow, Ph.D., Denise Brooks, Ph.D., Yaron Butterfield, B.S., Rebecca Carlsen, M.S., Scott Carter, Ph.D., Lynda Chin, M.D., Andy Chu, B.S., Eric Chuah, B.S., Kristian Cibulskis, B.S., Amanda Clarke, Simon G. Coetzee, Noreen Dhalla, B.S., Tim Fennell, M.S., Sheila Fisher, M.B.A., Stacey Gabriel, Ph.D., Gad Getz, Ph.D., Richard Gibbs, Ph.D., Ranabir Guin, B.S., Angela Hadjipanayis, Ph.D., D. Neil Hayes, M.D., M.P.H., Toshinori Hinoue, Ph.D., Katherine Hoadley, Ph.D., Robert A. Holt, Ph.D., Alan P. Hoyle, B.S., Stuart R. Jefferys, Ph.D., Steven Jones, Ph.D., Corbin D. Jones, Ph.D., Raju Kucherlapati, Ph.D., Phillip H. Lai, B.S., Eric Lander, Ph.D., Semin Lee, Ph.D., Lee Lichtenstein, M.S., Yussanne Ma, Ph.D., Dennis T. Maglinte, M.S., Harshad S. Mahadeshwar, M.S., Marco A. Marra, Ph.D., Michael Mayo, B.S., Shaowu Meng, Ph.D., Matthew L. Meyerson, M.D., Ph.D., Piotr A. Mieczkowski, Ph.D., Richard A. Moore, Ph.D., Lisle E. Mose, B.S., Andrew J. Mungall, Ph.D., Angeliki Pantazi, M.D., Ph.D., Michael Parfenov, M.D., Ph.D., Peter J. Park, Ph.D., Joel S. Parker, Ph.D., Charles M. Perou, Ph.D., Alexei Protopopov, Ph.D., Xiaojia Ren, M.A., M.S., Jeffrey Roach, Ph.D., Thaïs S. Sabedot, B.S., Jacqueline Schein, M.S., Steven E. Schumacher, M.S., Jonathan G. Seidman, Ph.D., Sahil Seth, M.S., Hui Shen, Ph.D., Janae V. Simons, B.S., Payal Sipahimalani, M.S., Matthew G. Soloway, B.S., Xingzhi Song, Ph.D., Huandong Sun, M.S., Barbara Tabak, Ph.D., Angela Tam, B.S., Donghui Tan, M.S., Jiabin Tang, Ph.D., Nina Thiessen, M.S., Timothy Triche, Jr., Ph.D., David J. Van Den Berg, Ph.D., Umadevi Veluvolu, M.Phil., Scot Waring, Ph.D., Daniel J. Weisenberger, Ph.D., Matthew D. Wilkerson, Ph.D., Tina Wong, B.S., Junyuan Wu, M.S., Liu Xi, M.S., Andrew W. Xu, Ph.D., Lixing Yang, Ph.D., Travis I. Zack, B.A., Jianhua Zhang, Ph.D., B. Arman Aksoy, Ph.D., Harindra Arachchi, B.S., M.B.A., Chris Benz, M.D., Brady Bernard, Ph.D., Daniel Carlin, Ph.D., Juok Cho, Ph.D., Daniel DiCara, M.S., Scott Frazer, Gregory N. Fuller, M.D., Ph.D., JianJiong Gao, Ph.D., Nils Gehlenborg, Ph.D., David Haussler, Ph.D., David I. Heiman, B.S., Lisa Iype, Ph.D., Anders Jacobsen, Ph.D., Zhenlin Ju, Ph.D., Sol Katzman, Ph.D., Hoon Kim, Ph.D., Theo Knijnenburg, Ph.D., Richard Bailey Kreisberg, M.S., Michael S. Lawrence, Ph.D., William Lee, Ph.D., Kalle Leinonen, M.S., Pei Lin, M.D., M.S., Shiyun Ling, Ph.D., Wenbin Liu, M.S., Yingchun Liu, Ph.D., Yuexin Liu, Ph.D., Yiling Lu, M.D., Gordon Mills, M.D., Ph.D., Sam Ng, B.S., Michael S. Noble, M.S., Evan Paull, B.S., Arvind Rao, Ph.D., Sheila Reynolds, Ph.D., Gordon Saksena, M.Eng., Zack Sanborn, Ph.D., Chris Sander, Ph.D., Nikolaus Schultz, Ph.D., Yasin Senbabaoglu, Ph.D.,

Ronglai Shen, Ph.D., Ilya Shmulevich, Ph.D., Rileen Sinha, Ph.D., Josh Stuart, Ph.D., S. Onur Sumer, M.S., Yichao Sun, M.S., Natalie Tasman, B.A., Barry S. Taylor, Ph.D., Doug Voet, M.S., Nils Weinhold, Ph.D., John N. Weinstein, M.D., Ph.D., Da Yang, M.D., Ph.D., Kosuke Yoshihara, M.D., Ph.D., Siyuan Zheng, Ph.D., Wei Zhang, Ph.D., Lihua Zou, Ph.D., Ty Abel, M.D., Ph.D., Sara Sadeghi, Ph.D., Mark L. Cohen, M.D., Jenny Eschbacher, M.D., Eyas M. Hattab, M.D., Aditya Raghunathan, M.D., Matthew J. Schniederjan, M.D., Dina Aziz, M.S., Gene Barnett, M.D., M.B.A., Wendi Barrett, B.A., Darell D. Bigner, M.D., Ph.D., Lori Boice, B.S., Cathy Brewer, R.N., Chiara Calatozzolo, B.S., Benito Campos, M.D., Carlos Gilberto Carlotti, Jr., M.D., Ph.D., Timothy A. Chan, M.D., Ph.D., Lucia Cuppini, Ph.D., Erin Curley, M.B.A., Stefania Cuzzubbo, M.D., Karen Devine, R.N., B.S.N., Francesco DiMeco, M.D., Rebecca Duell, J. Bradley Elder, M.D., Ashley Fehrenbach, B.S., Gaetano Finocchiaro, M.D., William Friedman, M.D., Jordonna Fulop, A.S.N., R.N., Johanna Gardner, C.T.R., Beth Hermes, B.A., Christel Herold-Mende, Ph.D., Christine Jungk, M.D., Ady Kendler, M.D., Norman L. Lehman, M.D., Eric Lipp, B.S., Ouida Liu, B.S., Randy Mandt, B.A., Mary McGraw, A.S.N., Roger Mclendon, M.D., Christopher McPherson, M.D., Luciano Neder, M.D., Ph.D., Phuong Nguyen, M.B.A., Ardene Noss, B.A., Raffaele Nunziata, M.D., Quinn T. Ostrom, M.P.H., Cheryl Palmer, M.D., Alessandro Perin, M.D., Ph.D., Bianca Pollo, M.D., Alexander Potapov, M.D., Olga Potapova, Ph.D., W. Kimryn Rathmell, M.D., Ph.D., Daniil Rotin, M.D., Ph.D., Lisa Scarpace, M.S., Cathy Schilero, R.N., B.S.N., Kelly Senecal, B.S., Kristen Shimmel, B.S., Vsevolod Shurkhay, M.D., Suzanne Sifri, R.N., B.S.N., Rosy Singh, B.S., Andrew E. Sloan, M.D., Kathy Smolenski, R.N., B.S.N., Susan M. Staugaitis, M.D., Ph.D., Ruth Steele, B.S., Leigh Thorne, M.D., Daniela P.C. Tirapelli, Ph.D., Andreas Unterberg, M.D., Ph.D., Mahitha Vallurupalli, B.S., Yun Wang, M.A.S., Ronald Warnick, M.D., Felicia Williams, A.A.B., Yingli Wolinsky, Ph.D., M.B.A., Sue Bell, M.S., Mara Rosenberg, B.S., Chip Stewart, Ph.D., Franklin Huang, M.D., Ph.D., Jonna L. Grimsby, Ph.D., Amie J. Radenbaugh, B.S., and Jianan Zhang, M.S.

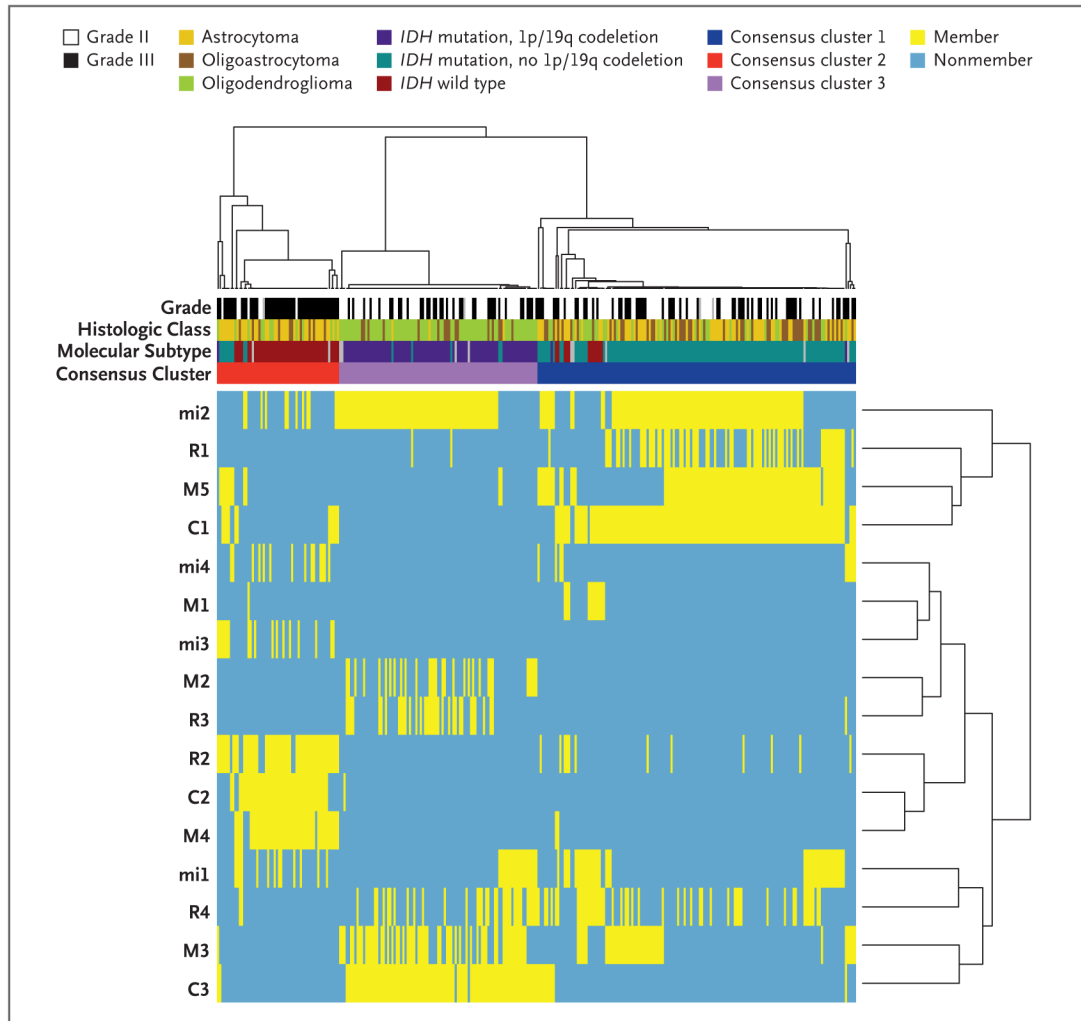


Figure 1. Cluster of Clusters (CoC) Analysis

The results of multiplatform analyses point to biologic subtypes defined by *IDH* mutation and 1p/19q codeletion status. CoC analysis uses the cluster assignments derived from individual molecular platforms to stratify tumors, thereby integrating data from analysis of messenger RNA (mRNA) (designated by R on the y axis), microRNA (mi), DNA methylation (M), and copy number (C). For each sample, membership in a particular cluster is indicated by a yellow tick, and nonmembership is indicated by a blue tick. CoC analysis resulted in a strong three-class solution, and a comparison of tracks for CoC consensus cluster with tracks for histologic and molecular class shows a stronger correlation with molecular class.

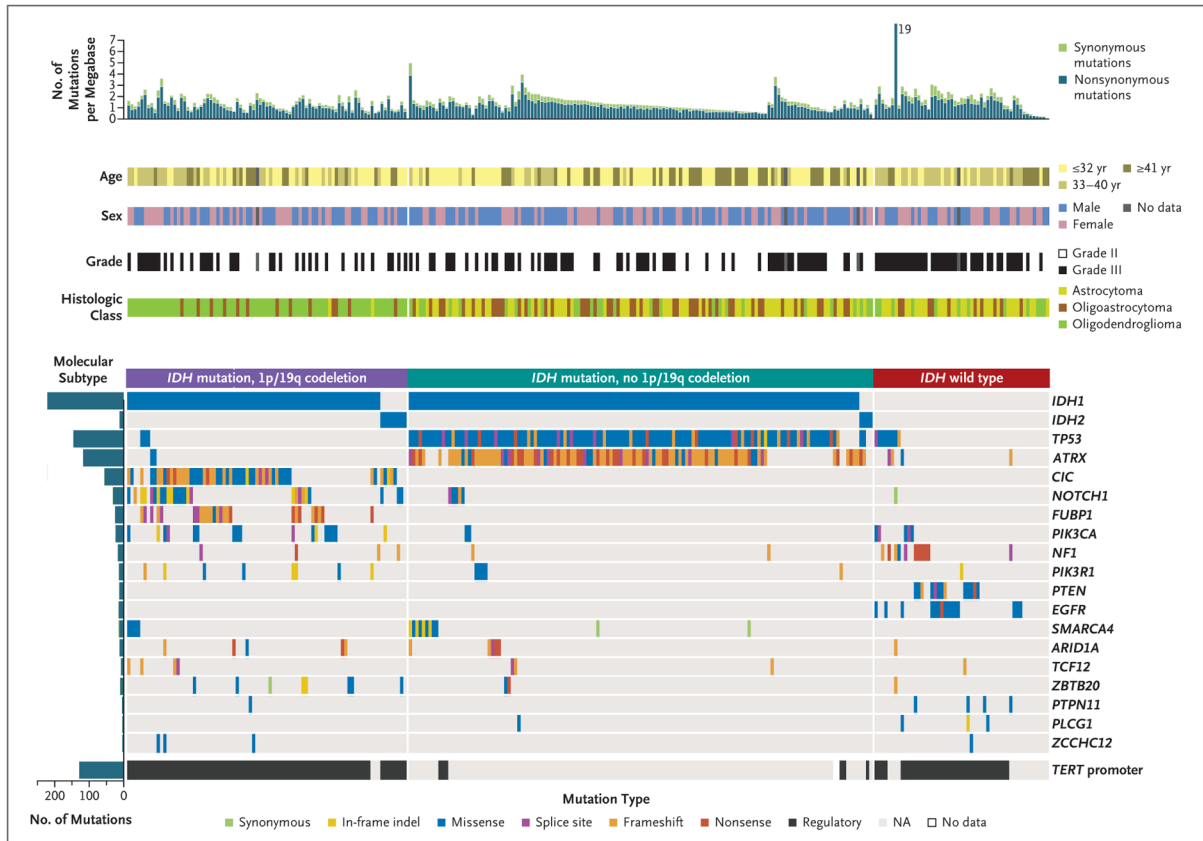


Figure 2. Mutational Landscape of Somatic Alterations in Lower-Grade Glioma

At the top of the figure, somatic mutation rates for each patient are stratified according to nonsynonymous (blue) and synonymous (green) mutations. In the middle portion of the figure, the clinical features associated with the patients are shown. At the bottom of the figure, genes that are significantly mutated (q value <0.1, determined with the use of the MutSig2CV algorithm) in lower-grade glioma are listed on the right. Samples from patients have been separated according to *IDH* mutation and 1p/19q codeletion status, with mutation types indicated in specific colors. NA denotes not applicable.

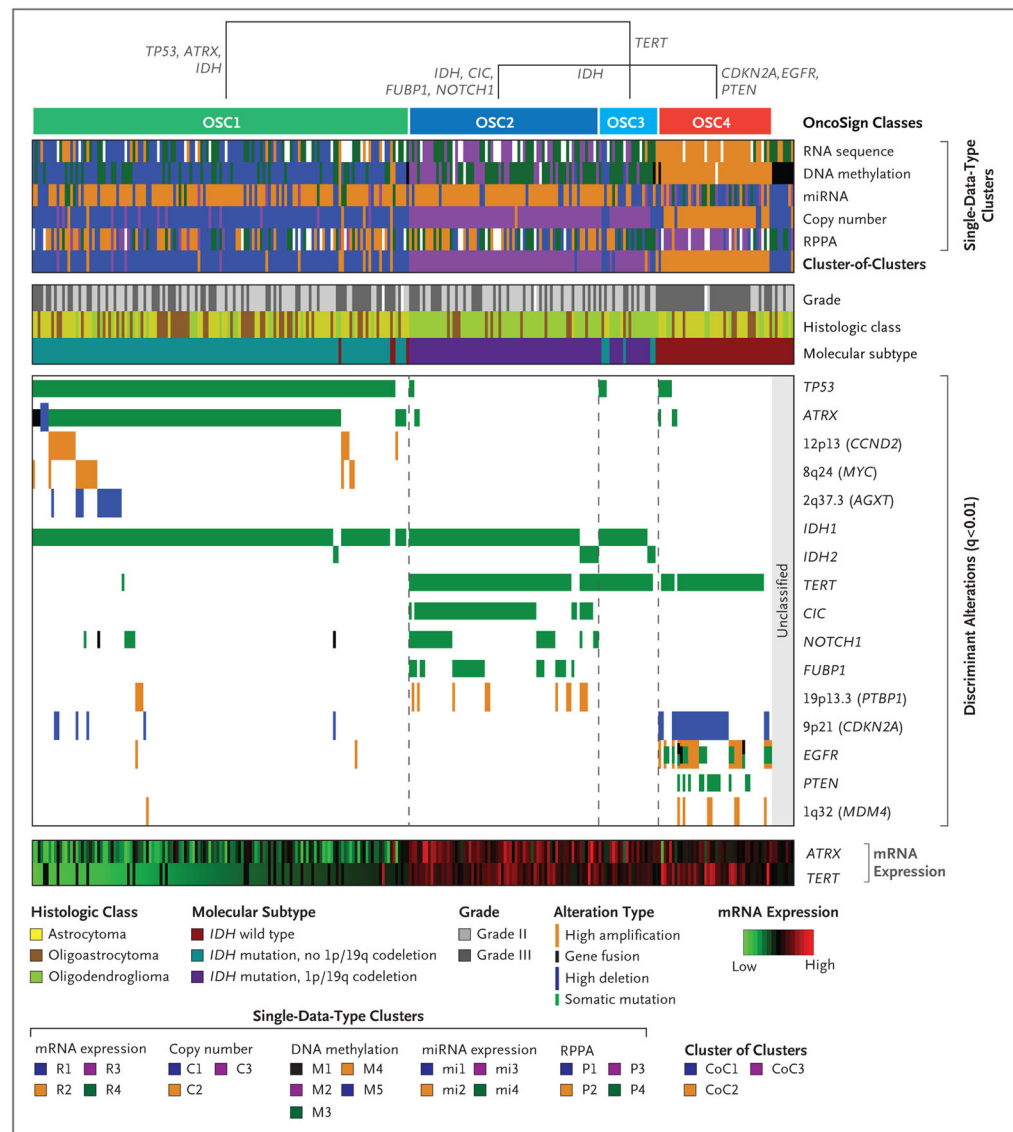


Figure 3. OncoSign Analysis

Four main classes (OncoSign classes [OSCs]) can be identified by means of unbiased clustering of tumors on the basis of recurrent copy-number alterations, mutations, and gene fusions. White indicates that no information was available. OSCs are largely consistent with the molecular subtypes identified on the basis of *IDH* mutation and 1p/19q codeletion status, and they also correlate with the results of single-platform analysis. Combinations of selected genomic events, termed oncogenic signatures, characterize each OSC. A small group of samples showed none of the recurrent events used in this analysis and were therefore categorized as unclassified. *TERT* promoter mutation and gene overexpression were found to be mutually exclusive with loss of *ATRX* and reduced gene expression, a finding consistent with the hypothesis that both alterations have a similar effect on telomere maintenance. The abbreviation miRNA denotes microRNA, and RPPA reverse-phase protein lysate array.

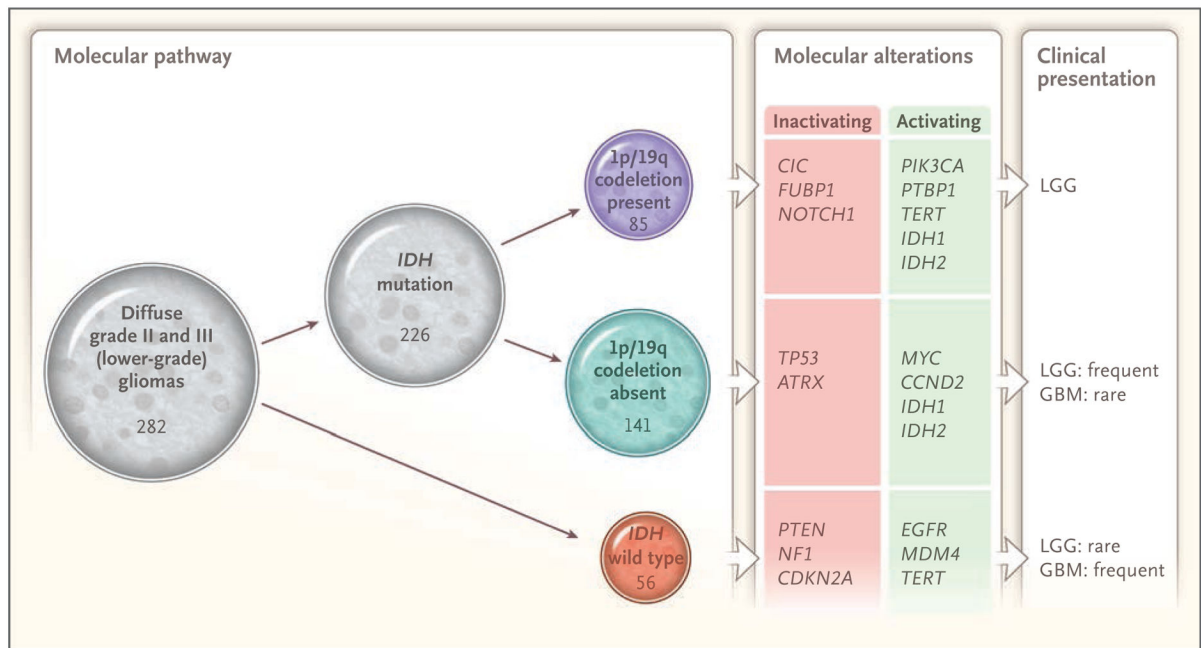


Figure 4. Summary of Major Findings

Shown is a schematic representation that summarizes the major molecular findings and conclusions of our study: consensus clustering yielded three robust groups that were strongly correlated with *IDH* mutation and 1p/19q codeletion status and had stereotypical and subtype-specific molecular alterations and distinct clinical presentations. GBM denotes glioblastoma, and LGG lower-grade glioma.

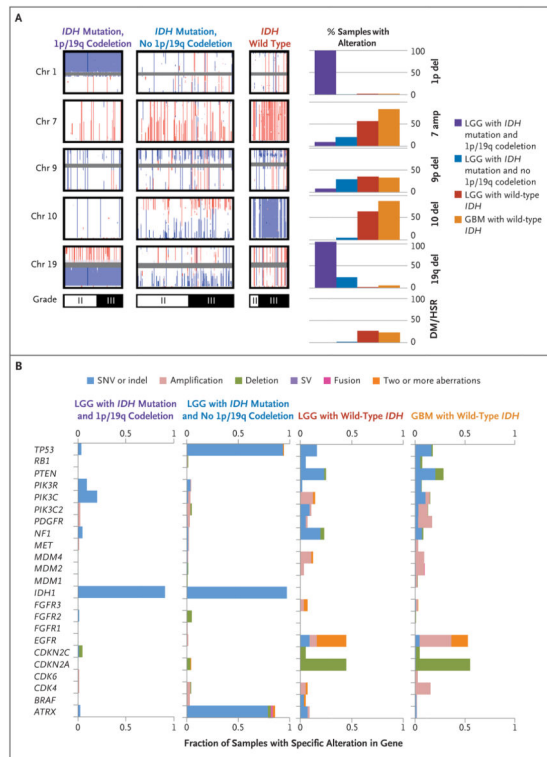


Figure 5. LGGs and GBMs with Wild-Type *IDH*

Panel A shows the frequency of large-scale copy-number alterations in specific molecular subtypes of LGG, which have been divided according to histologic grade. The University of California, Santa Cruz (UCSC), Cancer Genomics Browser³³ (<https://genome-cancer.ucsc.edu>) was used to visualize GISTIC thresholded copy-number calls across the indicated chromosomes. Each vertical line indicates the copy number for an individual sample, colored red (amplification), blue (deletion), or white (normal), at each genomic position. Percentages for the indicated copy-number alteration are shown in the bar graphs on the right. LGGs with wild-type *IDH* had frequencies of gains and losses similar to those of GBMs with wild-type *IDH* (from previously published Cancer Genome Atlas data²²) and were distinct from LGGs with mutated *IDH*. DM/HSR denotes double-minute chromosomes or homogeneously staining regions. Panel B shows the frequencies in the indicated LGG molecular subtypes of mutational events that are commonly found in GBM with wild-type *IDH*, including LGGs with *IDH* mutation and 1p/19q codeletion (85 samples), *IDH* mutation and no codeletion (141), and wild-type *IDH* (56). SNV denotes single-nucleotide variant, and SV structural variant. Differences in mutational frequency according to tumor grade are shown in Fig. S21 in Supplementary Appendix 1.

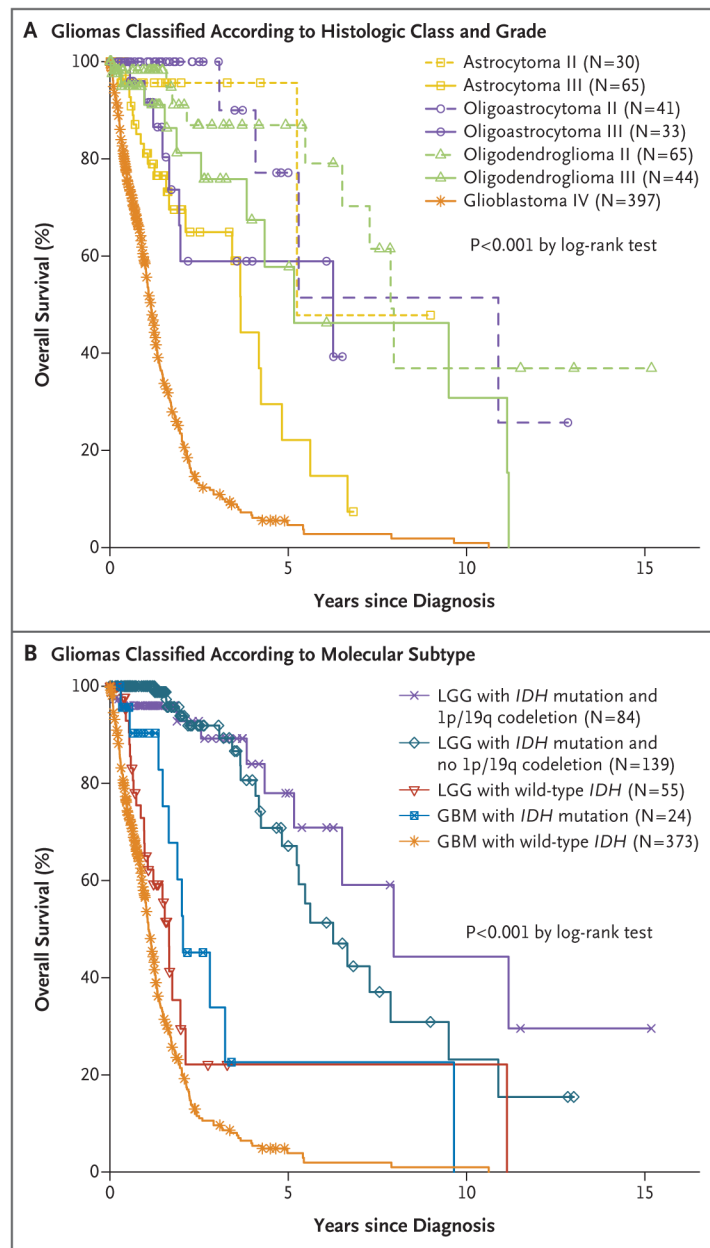


Figure 6. Clinical Outcomes

Panel A shows Kaplan–Meier estimates of overall survival among patients with LGGs that are classified according to traditional histologic type and grade. GBM samples (from previously published Cancer Genome Atlas data²²) are also included for comparison. Panel B shows overall survival among patients with LGGs that are classified according to *IDH* mutation and 1p/19q codeletion status. GBM samples classified according to *IDH* mutation status are also included. The results of an age-adjusted analysis are provided in Table S2 in Supplementary Appendix 1, and further division according to histologic type, grade, and molecular subtype is shown in Fig. S22 in Supplementary Appendix 1.

Table 1

Clinical Characteristics of the Sample Set According to *IDH* Mutation and 1p/19q Codeletion Status.*

Characteristic	Total (N = 278) [†]	<i>IDH</i> Mutation and 1p/19q Codeletion (N = 84)	<i>IDH</i> Mutation and No 1p/19q Codeletion (N = 139)	<i>IDH</i> Wild Type (N = 55)
Histologic type [‡] and grade [‡] — no. (%)				
Oligodendroglioma				
Grade II	65 (23)	38 (45)	21 (15)	6 (11)
Grade III	44 (16)	31 (37)	6 (4)	7 (13)
Oligoastrocytoma				
Grade II	41 (15)	9 (11)	30 (22)	2 (4)
Grade III	33 (12)	4 (5)	20 (14)	9 (16)
Astrocytoma				
Grade II	30 (11)	1 (1)	24 (17)	5 (9)
Grade III	65 (23)	1 (1)	38 (27)	26 (47)
Age at diagnosis — yr [‡]				
Mean	42.6±13.5	45.4±13.2	38.1±10.9	49.9±15.3
Range	14–75	17–75	14–70	21–74
Male sex — no. (%)	155 (56)	45 (54)	84 (60)	26 (47)
White race — no./total no. (%) [§]	261/274 (95)	79/81 (98)	131/138 (95)	51/55 (93)
Year of diagnosis — no. (%)				
Before 2005	38 (14)	10 (12)	18 (13)	10 (18)
2005–2009	88 (32)	30 (36)	44 (32)	14 (25)
2010–2013	152 (55)	44 (52)	77 (55)	31 (56)
Family history of cancer — no./total no. (%) [¶]				
None	108/190 (57)	30/58 (52)	64/98 (65)	13/34 (38)
Primary brain cancer	11/190 (6)	2/58 (3)	7/98 (7)	2/34 (6)
Other cancers	72/190 (38)	26/58 (45)	27/98 (28)	19/34 (56)
Extent of resection — no./total no. (%)				
Open biopsy	6/268 (2)	1/81 (1)	4/132 (3)	1/55 (2)
Subtotal resection	98/268 (37)	31/81 (38)	45/132 (34)	22/55 (40)
Gross total resection	164/268 (61)	49/81 (60)	83/132 (63)	32/55 (58)
Tumor location — no. (%) [‡]				
Frontal lobe	172 (62)	68 (81)	84 (60)	20 (36)
Parietal lobe	23 (8)	5 (6)	13 (9)	5 (9)
Temporal lobe	74 (27)	9 (11)	40 (29)	25 (45)
Other	9 (3)	2 (2)	2 (1)	5 (9)
Laterality — no./total no. (%)				
Left	133/276 (48)	37/84 (44)	69/137 (50)	27/55 (49)

Characteristic	Total (N = 278) [†]	<i>IDH</i> Mutation and 1p/19q Codeletion (N = 84)	<i>IDH</i> Mutation and No 1p/19q Codeletion (N = 139)	<i>IDH</i> Wild Type (N = 55)
Midline	5/276 (2)	2/84 (2)	2/137 (1)	1/55 (2)
Right	138/276 (50)	45/84 (54)	66/137 (48)	27/55 (49)
White matter — no./total no. (%)	74/144 (51)	26/48 (54)	37/72 (51)	11/24 (46)
First presenting symptom — no./total no. (%)				
Headache	64/252 (25)	15/72 (21)	39/129 (30)	10/51 (20)
Mental status change	22/252 (9)	7/72 (10)	10/129 (8)	5/51 (10)
Motor or movement change	18/252 (7)	6/72 (8)	7/129 (5)	5/51 (10)
Seizure	135/252 (54)	38/72 (53)	70/129 (54)	27/51 (53)
Sensory or visual change	13/252 (5)	6/72 (8)	3/129 (2)	4/51 (8)

* Plus–minus values are means \pm SD. Categorical distributions were compared with the use of Fisher’s exact test. Analysis of variance was used to compare age between groups.

[†] *IDH*–1p/19q status was not determined for 11 cases with clinical information.

[‡] $P < 0.01$ for the difference among the molecular subtypes.

[§] Race was self-reported. Of the 261 patients who reported their ethnic background, 5% identified themselves as Hispanic or Latino.

[¶] Included are patients for whom responses to questions regarding a family history of any cancer (192 patients) and a family history of primary brain cancer (197 patients) were available. $P < 0.05$ for the difference among the molecular subtypes.

^{//} One case (with wild-type *IDH*) was in the cerebellum, three cases were in the occipital lobe (two with *IDH* mutation and 1p/19q codeletion and one with an *IDH* mutation and no codeletion), and five cases were listed as “supratentorial, not otherwise specified” (one with an *IDH* mutation and no codeletion and four with wild-type *IDH*).